

# Calculation of atmospheric muons from cosmic gamma rays

J. Poirier<sup>1</sup>, S. Roesler<sup>2</sup>, and A. Fassò<sup>3</sup>

<sup>1</sup>Center for Astrophysics at Notre Dame, Physics Dept., University of Notre Dame, Notre Dame, Indiana 46556 USA

<sup>2</sup>Stanford Linear Accelerator Center, Stanford, California 94309 USA

<sup>3</sup>CERN-EP/AIP, CH-1211 Geneva 23, Switzerland

**Abstract.** The production of muons in atmospheric showers initiated by gamma rays with energies below 10 TeV is calculated using the Monte Carlo code FLUKA. The simulations as well as various general properties of the muons reaching sea level and of their ancestors in the cascade are discussed.

---

## 1 Introduction

Muons observed by ground-based cosmic ray experiments, such as MILAGRO (R. Atkins et al., 2000) or GRAND (Poirier et al., 1999), are mainly produced in showers initiated by cosmic ray protons and nuclei. A small fraction, however, originates from photonuclear reactions of primary cosmic gamma rays. Despite their relative scarcity, the latter contribution might be distinguished from the former due to the fact that cosmic gamma rays are not affected by magnetic fields and therefore point directly to the location of their source. Muons from cosmic gamma rays should thus be characterized by an accumulation around a particular angle. Their angular distribution at ground level is determined by various physical processes occurring during shower propagation in the atmosphere, such as inelastic interactions, Coulomb scattering or deflection by the magnetic field of the Earth. Experimental analysis of those accumulations of muons requires information on the angular distribution. Due to the complexity of the physical processes this can only be provided by detailed Monte Carlo simulations.

The present paper discusses simulations of atmospheric showers initiated by gamma rays with energies below 10 TeV using the Monte Carlo code FLUKA. In addition, various general properties of the muons reaching sea level and of their ancestors in the cascade are presented. Angular distributions of muons are discussed in a separate contribution to this meeting (Poirier et al., 2001).

---

*Correspondence to:* J. Poirier (poirier@nd.edu)

## 2 The FLUKA calculations

The 2000 version of the FLUKA Monte Carlo code (Fassò et al., 2000a,b) was used to simulate the electromagnetic and hadronic particle cascades induced by primary gamma rays in the atmosphere. The powerful biasing capabilities of the code allowed a simulation of the full three-dimensional shower in a single run from the top of the atmosphere down to ground level.

The physical models implemented in FLUKA which are relevant for the present study are discussed in Fassò and Poirier (2001). It should be emphasized that all models were validated by comprehensive comparisons of FLUKA results with experimental data obtained mostly at accelerators but also in recent cosmic ray studies (see references in Fassò and Poirier (2001)).

In order to study the dependence of the shower properties on the primary photon energy, the showers were calculated for monoenergetic photons impinging vertically on top of the atmosphere (taken to be 80 km above sea level). In total, 9 sets of simulations were performed for the following primary energies: 1, 3, 10, 30, 100, 300, 1000, 3000, and 10000 GeV. The atmosphere was approximated by 50 layers with a constant density in each layer and with layer densities decreasing exponentially with increasing altitude.

The use of variance reduction (biasing) techniques was essential to obtain results with reasonable statistical significance. They included leading particle biasing at each electromagnetic interaction, biasing of the photon mean-free-path with respect to photonuclear interactions, biasing of the decay length of charged mesons, and particle splitting at the boundaries of different air layers. Each of these biasing techniques alters the statistical weight of a particle in the cascade. A muon as produced and transported in the Monte Carlo simulation and which carries a certain statistical weight (hereafter called “MC muon”) contributes to distributions, yields, etc., of actual, measurable muons with a probability equal to its weight. The use of biasing techniques would not be appropriate to study fluctuations within the same shower which,

*27th International Cosmic Ray Conference (ICRC 2001)  
7-15 Aug 2001, Hamburg, Germany*

however, is not the aim of this study.

For each MC muon reaching sea level (detection level) the following information was recorded in a file for later analysis:

1. Information on the muon at detection level: muon charge, lateral coordinates  $(x, y)$  with respect to shower axis  $(z)$ , direction cosines with respect to the  $x$  and  $y$  axes, kinetic energy, statistical weight of the muon, and number of the event (i.e., primary cosmic ray photon) which produced this muon.
2. Information on the muon at its production vertex (i.e., meson decay vertex): lateral coordinates  $(x, y)$  with respect to shower axis, direction cosines with respect to the  $x$  and  $y$  axes, height  $z$ , kinetic energy, statistical weight of the muon, and identity of the decaying meson.
3. Information on the grandparent at the parent production vertex: particle identity, lateral coordinates  $(x, y)$  with respect to shower axis, direction cosines with respect to the  $x$  and  $y$  axes, height  $z$ , kinetic energy, statistical weight of the particle, and generation number.
4. Information on the photonuclear interaction vertex preceding the hadronic cascade in which the muon at detection level has been created: lateral coordinates  $(x, y)$  with respect to shower axis, direction cosines with respect to the  $x$  and  $y$  axes, height  $z$ , energy, statistical weight of the photon, and generation number of the photon

The generation of a particle increases with each sampled discrete interaction (electromagnetic or hadronic), i.e., the primary photon is generation “1,” the generation of the electron and positron after the first pair production process would be “2,” etc. Delta ray production and Coulomb scattering are not considered to increase the generation number.

A summary of the simulated particles cascades for each primary gamma ray energy is given in Table 1. In the following, all results refer to the sum of positive and negative muons. The number of histories (number of primary gamma

**Table 1.** Summary of the simulated particle cascades.

$E_\gamma$ (GeV)	$N_\gamma$	$N_\mu$	$N_\mu/N_\gamma$
1	4542000	0.00378	$(8.32 \pm 0.46) \times 10^{-10}$
3	26000000	117.7	$(4.53 \pm 0.23) \times 10^{-6}$
10	2250000	1191	$(5.29 \pm 0.03) \times 10^{-4}$
30	1260000	3843	$(3.05 \pm 0.01) \times 10^{-3}$
100	800000	11351	$(1.42 \pm 0.01) \times 10^{-2}$
300	324445	17259	$(5.32 \pm 0.02) \times 10^{-2}$
1000	143131	31709	$(2.22 \pm 0.01) \times 10^{-1}$
3000	27040	21954	$(8.12 \pm 0.05) \times 10^{-1}$
10000	18000	58874	$3.27 \pm 0.03$

rays),  $N_\gamma$ , calculated for each primary energy decreases with increasing energy in order to obtain uniform statistical significance on the muons which reach ground level for the different primary energies. At the lowest energy (1 GeV) the muon flux per gamma at sea level is very small so that even with a significant amount of biasing in the simulations it is difficult to reach adequate statistics. Less emphasis was therefore put on the simulation at 1 GeV. The column  $N_\mu$  gives the total number of muons (i.e., the sum of the weights) reaching detection level for the given number of primary photons  $N_\gamma$ . The predictions for the muon multiplicity at sea level per incident primary gamma ray  $N_\mu/N_\gamma$  are listed in the last column of Table 1.

### 3 Properties of muon production in gamma ray showers

#### 3.1 The ancestors of the muons

Table 2 shows which parent contributes through its decay to the detected muons for the different primary gamma ray energies. At the lowest energy (1 GeV) about 89% of the

**Table 2.** Fractional contributions to the parents of the muons which reach sea level.

$E_\gamma$ (GeV)	$\pi^+$	$\pi^-$	$K^+$	$K^-$	neutral kaons
1	0.106	0.894	0.0	0.0	0.0
3	0.495	0.485	0.020	0.0	$1.7 \times 10^{-4}$
10	0.492	0.489	0.011	0.007	$9.8 \times 10^{-4}$
30	0.482	0.482	0.019	0.014	$3.1 \times 10^{-3}$
100	0.478	0.477	0.022	0.018	$4.4 \times 10^{-3}$
300	0.477	0.476	0.023	0.019	$4.7 \times 10^{-3}$
1000	0.475	0.476	0.024	0.019	$5.2 \times 10^{-3}$
3000	0.476	0.475	0.025	0.020	$5.1 \times 10^{-3}$
10000	0.474	0.477	0.024	0.020	$5.2 \times 10^{-3}$

muons are produced in decays of negative pions and 11% in decays of positive pions. This asymmetry can be explained by the different interaction cross sections at low energy of pions of either charge and by the fact that these pions are mainly produced in secondary interactions of neutrons (see below). Correspondingly, the probability for positive pions to interact instead of decay is larger than for negative pions. Above 3 GeV this asymmetry disappears and decaying kaons begin to contribute to the sea level muon flux. The latter contribution increases with energy and amounts to about 5% at 10 TeV.

It is interesting to note that at all energies FLUKA predicts the relative contribution of a positive kaon parent to be always larger than that of a negative kaon by about 20%. This effect is due to the properties of the Dual Parton Model describing inelastic hadronic interactions within FLUKA. In particular, it is a feature of the Reggeon contribution which describes particle production by one quark-diquark string stretched between a valence quark of the fluctuating photon

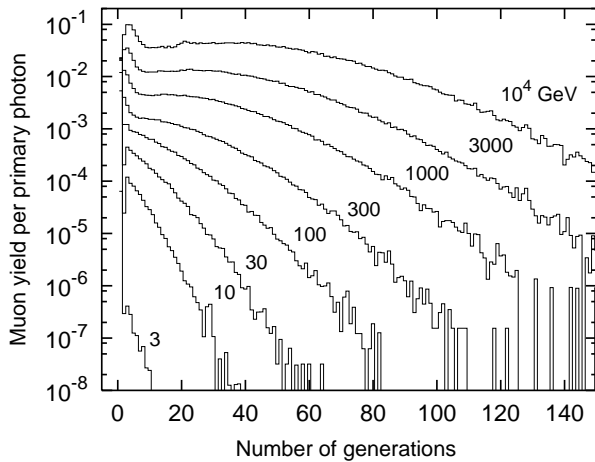


**Fig. 1.** Distribution in the number of generations in the shower carried by the particles creating the parent meson.

(Vector Meson Dominance model) and a diquark of a target nucleon. In this picture, kaon production involves the creation of a  $s\bar{s}$  quark-antiquark pair and, in case of negative kaons, also the creation of an  $u\bar{u}$  pair. On the other hand, positive kaons can be readily formed also by a  $u$ -quark of the fluctuating photon leading to the observed asymmetry.

The fractional contribution to the muon's grandparent is given in Table 3. The calculations for 1 GeV show distinctly different features. About 97% of the muons at sea level originate from mesons produced in interactions of neutrons in the close vicinity of the detector. At all other energies photoproduction dominates the picture with a contribution decreasing with energy from 99% at 3 GeV to 60% at the highest energy; the remaining fraction is mainly from pions.

**Table 3.** Fractional contributions to the grandparent of the detected muon at sea level.

$E_\gamma$ (GeV)	$\gamma$	p and $\bar{p}$	n and $\bar{n}$	$\pi^+$	$\pi^-$
1	0.0017	0.023	0.97	0.00078	0.0049
3	0.99	0.00039	0.005	0.0023	0.0021
10	0.99	0.00082	0.0019	0.0026	0.0027
30	0.97	0.0041	0.0053	0.0093	0.0092
100	0.91	0.014	0.015	0.026	0.027
300	0.83	0.025	0.026	0.056	0.056
1000	0.73	0.037	0.041	0.091	0.090
3000	0.65	0.049	0.049	0.12	0.12
10000	0.60	0.054	0.057	0.13	0.14

### 3.2 Distributions of the number of generations

The distributions of the generation number of the grandparent of the sea level muon is shown in Fig. 1. The lower the energy of the primary gamma ray the smaller is the atmospheric shower resulting in a relatively narrow distribu-

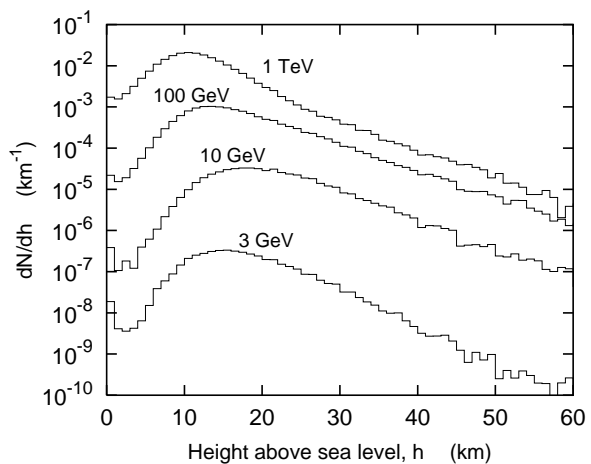


**Fig. 2.** Distribution of the muon production heights. Results are normalized per primary photon. The top of the atmosphere is at 80 km in the calculations.

tion. This distribution is peaked at generation one for energies below a few hundred GeV where the parent is mainly produced in a photoproduction process of the primary photon (see also Table 3). At higher energies secondary hadron interactions contribute significantly to the production of the parent. These secondary hadrons are mainly of third or fourth generation and cause a shift of the peak of the total distribution at TeV energies. The large tail at these energies which extends up to more than 100 generations reflects photoproduction processes of secondary photons in the large electromagnetic shower.

### 3.3 The muon production heights

The distributions of heights above sea level at which the detected muons were produced are shown for four primary energies in Fig. 2. As expected, at high energy there is a decrease in height with increasing energy of the primary gamma ray because of the logarithmic increase of the shower length. However, as the energy of the primary gamma ray decreases below 10 GeV, the energy of the muon parent is close to the minimum energy required for the muon to penetrate the blanket of air between its production and sea level. Hence, the most probable height of muon production begins to decrease with energies decreasing below 10 GeV. The blip-up near zero height, most pronounced in the 3 and 10 GeV distributions, represents the excess contribution from very low energy muons.

### 3.4 Radial distributions

The radial distributions of the muons at their production vertices and at sea level are shown in Fig. 3 for five different gamma ray energies. The radial distance,  $R$ , is defined with respect to the shower axis ( $z$  axis). The quantity  $dN/dA$  denotes the number of muons per unit area and per primary gamma ray. The radial distributions of the production ver-

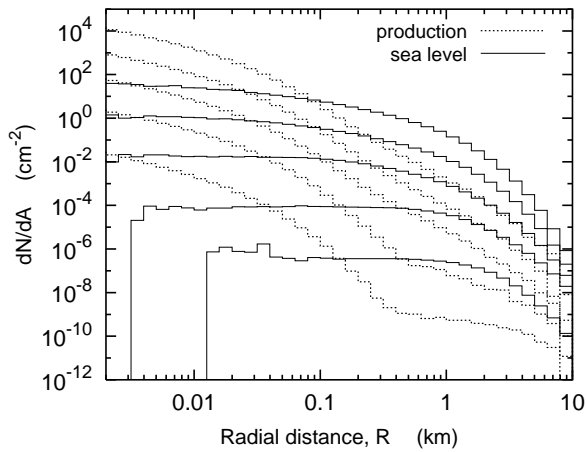


**Fig. 3.** Radial distribution of the muon production vertices (i.e. meson decay vertices, dotted histograms) and of the muons at sea level (solid histograms). Results are given for primary photon energies of 3, 10, 100,  $10^3$ , and  $10^4$  GeV, respectively (from the bottom curve to the top). Values have been normalized per primary photon.

tices are labeled “production.”

All distributions extend to more than 10 km. Whereas the sea level distributions have a relatively flat shape below  $R = 2$  km, the production vertex distributions are increasing toward the shower axis and exhibit a change in slope or discontinuity at about 500 m which is most pronounced at low primary energy. This discontinuity is due to the superposition of mesons produced in photoproduction processes which dominate at small radii and of mesons produced by interactions of nucleons or other hadrons constituting the tail at large  $R$ .

### 3.5 Energy distribution of the muons

The kinetic energy distributions of muons at sea level and at the production vertex of these muons are shown in Fig. 4. Note that the distributions are multiplied by the muon energy  $E_\mu$  in order to better show possible spectral structures at the higher energies. Whereas the sea level spectra are a smooth function of energy, the distributions of the muon energies at their birth exhibit a two-component structure. This two-component structure is again due to the superposition of muons from mesons generated in photoproduction processes and those generated by interacting hadrons.

## 4 Summary

General properties of muon production in atmospheric gamma ray showers were studied in detailed Monte Carlo simulations using FLUKA. Sophisticated biasing techniques available in FLUKA made it possible to obtain results with good statistical accuracy for a wide range of primary energies.

As expected, most of the muons which reach sea level are decay products of charged pions; the contribution from kaons increases as the primary energy increases. Below 100 GeV

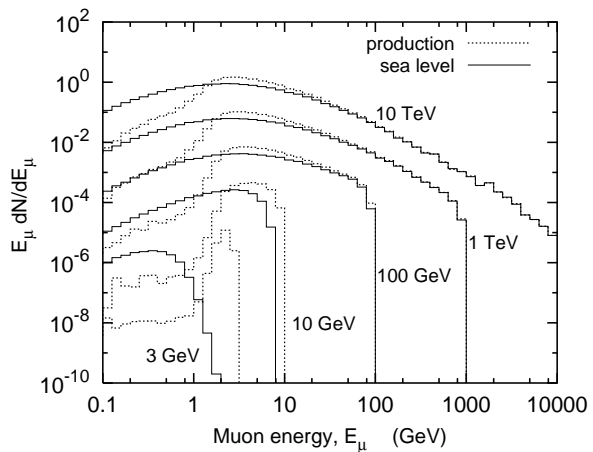


**Fig. 4.** Kinetic energy spectra of muons at their production vertices (dotted histograms) and at sea level (solid histograms). Values are normalized per primary photon.

primary energy, the decaying mesons are produced mainly in photoproduction processes (except at very low energies, i.e. below about 1 GeV). At higher energies, hadronic interactions of nucleons and pions begin to contribute significantly. The distribution of the number of generations becomes wider with increasing primary energy and extends up to more than 100 generations, reflecting the complexity of the problem. The distribution of the heights where the observed muons are produced shows a maximum between 10 and 20 km. The position of the maximum depends on the primary gamma ray energy and decreases with increasing energy above a primary energy of about 10 GeV.

*Acknowledgements.* Part of this work was supported by the Department of Energy under contract DE-AC02-76SF00515. Project GRAND is funded through grants from the University of Notre Dame and private donations.

## References

- Atkins, R. *et al.*, Nucl. Instr. Meth. in Phys. Res. A **449**, 478, 2000.
- Fassò, A., Ferrari, A., and Sala, P.R., *Electron-photon Transport in FLUKA: Status*, to appear in *Proceedings of the International Conference on Advanced Monte Carlo for Radiation Physics, Particle Transport Simulation and Applications, Monte Carlo 2000*, Lisbon, Portugal, 2000a.
- Fassò, A. *et al.*, *FLUKA: Status and Perspectives for Hadronic Applications*, to appear in *Proceedings of the International Conference on Advanced Monte Carlo for Radiation Physics, Particle Transport Simulation and Applications, Monte Carlo 2000*, Lisbon, Portugal, 2000b.
- Fassò, A. and Poirier, J., Phys. Rev. D **63**, 036002, 2001.
- Poirier, J. *et al.*, *Proceedings of the 26th International Cosmic Ray Conference (ICRC)*, Vol. 5, p. 304, 1999.
- Poirier, J., Roesler, S., and Fassò, A., *Muon angles at sea level from cosmic gamma rays below 10 TeV*, presented at this meeting by J. Poirier, 2001.